# Supplementary Fig. S1

| Parameter | H1781 | H1781DSR3 |
|---|---|---|
| Mapped reads (million) | 21.3 | 19.2 |
| On-target reads (%) | 98.8 | 98.8 |
| Mean sequencing depth | 1,389 | 1,253 |
| Coverage uniformity (%) | 95.0 | 94.9 |
| ERBB2 median depth | 1,657 | 1,615 |
| ERBB2 median depth, excluding low-coverage region | 1,684.5 | 1,621.5 |
| ERBB2 depth range, excluding low-coverage region | 376–3,704 | 271–3,224 |
| TOP1 median depth | 1,709 | 1,300 |
| TOP1 depth range | 438–3,232 | 367–2,652 |

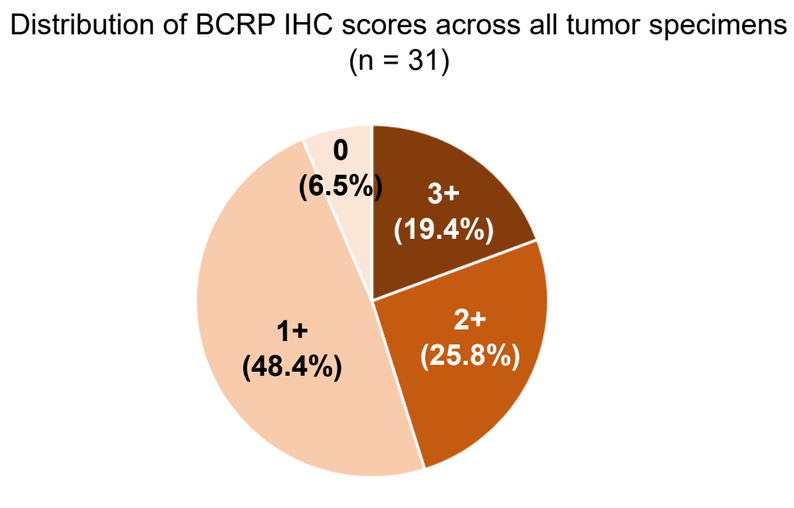
**Supplemental Figure S1**
Sequencing quality metrics and coverage of ERBB2 and TOP1 in H1781 and H1781DSR3 cells. A region of relatively low sequencing coverage was identified at chr17:37,856,539–37,856,660 (hg19/GRCh37), spanning the ERBB2 exon 1–intron 1 boundary. ERBB2 sequencing depth values excluding this region are presented separately.

# Supplementary Fig. S2

| ID | Gene Symbol | Fold Change | P-val | FDR P-val |
|---|---|---|---|---|
| TC0200015645.hg.1 | ABCA12 | 134.25 | 1.42E-06 | 0.0013 |
| TC0400011279.hg.1 | ABCG2 | 12.49 | 2.18E-05 | 0.0044 |
| TC1700008263.hg.1 | ABCC3 | 7.48 | 0.0002 | 0.0131 |
| TC0200016774.hg.1 | ABCB6 | 5.47 | 4.76E-05 | 0.0066 |
| TC0300013360.hg.1 | ABCC5 | 4.1 | 0.0008 | 0.026 |
| TC1600007022.hg.1 | ABCC1 | 3.74 | 0.0004 | 0.0174 |
| TC0400008902.hg.1 | ABCE1 | 3.4 | 0.0007 | 0.025 |
| TC0700007479.hg.1 | ABCA13 | 2.8 | 0.0113 | 0.0948 |
| TC1600010216.hg.1 | ABCC11 | 2.61 | 0.002 | 0.0396 |
| TC0600008087.hg.1 | ABCC10 | 2.39 | 0.0122 | 0.0983 |
| TC0700013065.hg.1 | ABCF2 | 2.08 | 0.0042 | 0.0575 |
| TC0100009097.hg.1 | ABCD3 | 2.05 | 0.0348 | 0.1767 |
| TC1600009105.hg.1 | ABCA3 | 1.86 | 0.0069 | 0.0743 |
| TC1900006508.hg.1 | ABCA7 | 1.67 | 0.0329 | 0.1716 |
| TC0X00008795.hg.1 | ABCD1 | 1.6 | 0.0258 | 0.1489 |
| TC1700012460.hg.1 | ABCA5 | 1.56 | 0.0353 | 0.1782 |
| TC1700011574.hg.1 | ABCA8 | 1.55 | 0.0965 | 0.3128 |
| TC0600007535.hg.1 | ABCF1 | 1.41 | 0.0511 | 0.22 |
| TC0100017666.hg.1 | ABCB10 | 1.33 | 0.0933 | 0.3063 |
| TC1200012256.hg.1 | ABCB9 | 1.26 | 0.161 | 0.4126 |
| TC0200014848.hg.1 | ABCB11 | 1.23 | 0.342 | 0.6174 |
| TC0300009694.hg.1 | ABCF3 | 1.23 | 0.2882 | 0.5664 |
| TC0100014977.hg.1 | ABCA4 | 1.22 | 0.2383 | 0.5112 |
| TC0700011706.hg.1 | ABCB1 | 1.18 | 0.275 | 0.5529 |
| TC1600010215.hg.1 | ABCC12 | 1.13 | 0.4651 | 0.7191 |
| TC0200007402.hg.1 | ABCG8 | 1.13 | 0.4332 | 0.6937 |
| TC0700009690.hg.1 | ABCB8 | 1.11 | 0.6125 | 0.8228 |
| TC1100010237.hg.1 | ABCC8 | 1.11 | 0.4665 | 0.7199 |
| TC1000008628.hg.1 | ABCC2 | 1.06 | 0.7827 | 0.912 |
| TC1700011575.hg.1 | ABCA9 | 1.01 | 0.9384 | 0.978 |
| TC1100009242.hg.1 | ABCG4 | -1 | 0.9843 | 0.995 |
| TC1200010413.hg.1 | ABCD2 | -1.03 | 0.828 | 0.9335 |
| TC0200012417.hg.1 | ABCG5 | -1.08 | 0.6921 | 0.8675 |
| TC0700006852.hg.1 | ABCB5 | -1.09 | 0.6255 | 0.83 |
| TC0900012025.hg.1 | ABCA2 | -1.18 | 0.3082 | 0.5871 |
| TC0900011072.hg.1 | ABCA1 | -1.2 | 0.2593 | 0.5347 |
| TC1200010111.hg.1 | ABCC9 | -1.21 | 0.3108 | 0.5895 |
| TC1700012459.hg.1 | ABCA10 | -1.22 | 0.1951 | 0.4583 |
| TC1700011578.hg.1 | ABCA6 | -1.23 | 0.3906 | 0.6583 |
| TC0X00010099.hg.1 | ABCB7 | -1.23 | 0.2321 | 0.504 |
| TC1600009545.hg.1 | ABCC6 | -1.28 | 0.1392 | 0.3807 |
| TC1400009690.hg.1 | ABCD4 | -1.29 | 0.1206 | 0.3529 |
| TC2100007241.hg.1 | ABCG1 | -1.39 | 0.103 | 0.3233 |
| TC0700011705.hg.1 | ABCB4 | -1.64 | 0.0172 | 0.1189 |
| TC1300009505.hg.1 | ABCC4 | -1.82 | 0.009 | 0.0844 |

**Supplemental Figure S2**
Differential expression of ATP-binding cassette (ABC) transporter family genes between T-DXd-resistant H1781DSR3 and parental H1781 cells. Gene expression was analyzed using the Clariom S Human Array with two biological replicates per cell line. Fold changes represent gene expression levels in H1781DSR3 cells relative to parental H1781 cells. Positive and negative fold-change values indicate increased and decreased expression in H1781DSR3 cells, respectively. P values were calculated using ANOVA in Transcriptome Analysis Console software (version 4.0.3), and false discovery rate (FDR)-adjusted P values are provided to account for multiple testing. Genes are listed in descending order of fold change.

# Supplementary Fig. S3




**Supplemental Figure S3**
Distribution of BCRP IHC scores across all tumor specimens. All available tumor specimens were included, including multiple specimens from individual patients where applicable (n = 31).

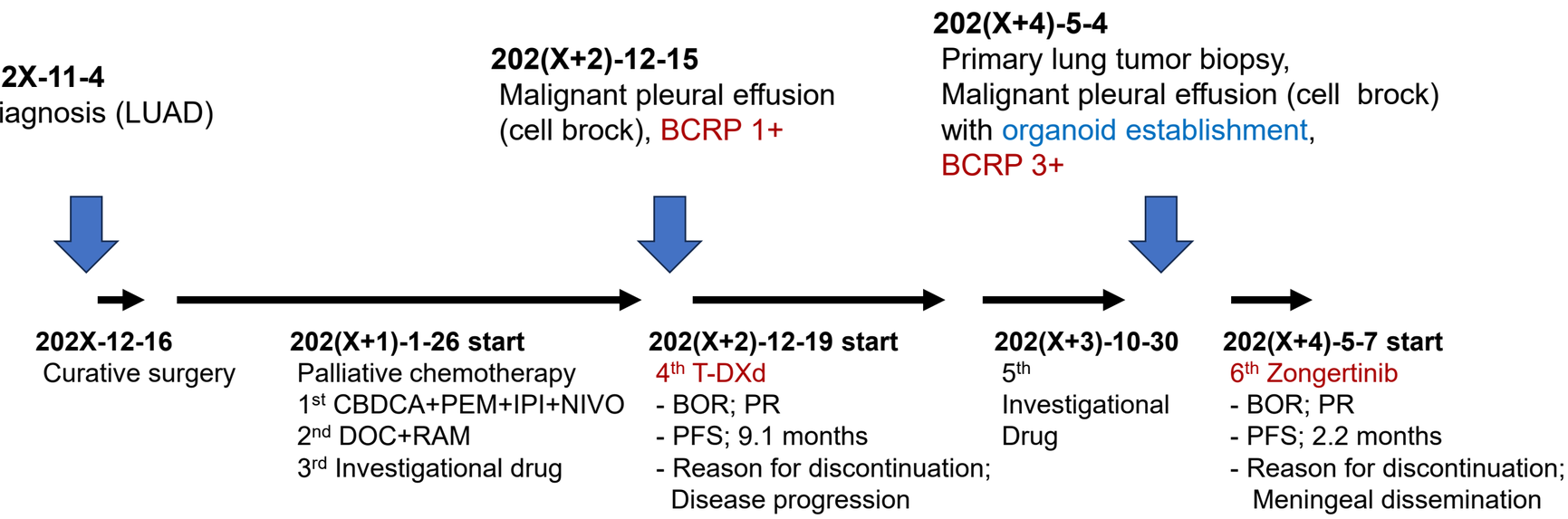
# Supplementary Fig. S4

| Patient No. | Sex | Age | Mutation type | BOR to T-DXd | PFS on T-DXd (months) | Ongoing T-DXd treatment at data cutoff | Prior systemic therapy before T-DXd | Specimen type | Specimen collection timing |
|---|---|---|---|---|---|---|---|---|---|
| 1 | Female | 48 | G770_A771ins | SD | 11.7 | No | No | 1. Primary lung tumor (biopsy)<br>2 Liver metastasis (biopsy) | 1.Before T-DXd<br>2. After T-DXd |
| 2 | Female | 50 | G776delinsVC | PR | 10.7 | No | Yes (Chemo, IC) | 1. Primary lung tumor (biopsy)<br>2 Liver metastasis (biopsy) | 1.Before systemic therapy<br>2. After T-DXd |
| 3 | Male | 68 | E770_A771ins | PR | 9.1 | No | Yes (Chemo, ICI, Investigational drug) | 1. Malignant pleural effusion (cell block)<br>2. Primary lung tumor (biopsy) | 1. Before T-DXd<br>2. After T-DXd and subsequent chemotherapy, before zongertinib |
| 4 | Male | 56 | G770_A771ins | SD | 9.3 | No | Yes (Chemo, ICI) | 1. Primary lung tumor biopsy<br>2. Primary lung tumor (biopsy) | 1.Before systemic therapy<br>2. After T-DXd |
| 5 | Male | 78 | A775-G776insYVMA | PR | 6.5 | No | Yes (Chemo) | 1. Malignant pleural effusion (cell block)<br>2 Primary lung tumor (biopsy) | 1. Before T-DXd<br>2. After T-DXd and subsequent chemotherapy, before zongertinib |
| 6 | Male | 68 | A775-G776insYVMA | SD | 8.6 | Yes | Yes (Chemo, ICI) | Primary lung tumor (surgical resection) | Before systemic therapy |
| 7 | Female | 41 | A775-G776insYVMA | PR | 6.2 | No | Yes (Chemo, ICI) | Primary lung tumor (biopsy) | Before T-DXd |
| 8 | Female | 33 | G770_A771insAYVM | PR | 16.5 | Yes | Yes (Chemo, ICI) | Lung metastasis (surgical resection) | Before systemic therapy |
| 9 | Female | 69 | G770_A771insAYVM | SD | 11.1 | No | Yes (Chemo, ICI) | Primary lung tumor (biopsy) | Before systemic therapy |
| 10 | Female | 77 | G770_A771insAYVM | PD | 1.4 | No | Yes (Chemo, ICI) | Primary lung tumor (surgical resection) | Before systemic therapy |
| 11 | Female | 42 | G776delinsVC | SD | 4.4 | No | Yes (Chemo, ICI) | Primary lung tumor (biopsy) | Before systemic therapy |
| 12 | Male | 69 | G770_A771ins | PR | 17.5 | Yes | Yes (Chemo, ICI) | Lymph node metastasis (surgical resection) | Before systemic therapy |
| 13 | Male | 71 | A771-Y772insYVMA | PD | 1.5 | No | Yes (Chemo, ICI) | Primary lung tumor (surgical resection) | Before systemic therapy |
| 15 | Female | 53 | G778_P780insGSP | SD | 3.2 | No | Yes (Chemo, ICI) | Primary lung tumor (biopsy) | Before systemic therapy |
| 16 | Male | 61 | A775-G776insYVMA | PR | 3.7 | No | Yes (Chemo) | Malignant pleural effusion (cell block) | Before T-DXd |
| 20 | Male | 59 | A775_G776insYVMA | PR | 6.9 | Yes | Yes (Chemo, ICI) | Malignant pleural effusion (cell block) | Before systemic therapy |
| 21 | Male | 64 | A775_G776insYVMA | PR | 14 | No | Yes | Primary lung tumor (biopsy) | Before systemic therapy |
| 22 | Male | 80 | G776delinsVC | PR | 13.4 | No | Yes | 1. Primary lung tumor (surgical resection)<br>2. Malignant pleural effusion (cell block) | 1. Before systmic therapy<br>2. After T-DXd |
| 23 | Male | 76 | A775_G776insYVMA | PR | 8.4 | No | Yes | Primary lung tumor (biopsy) | Before T-DXd |
| 24 | Male | 64 | A775_G776insYVMA | PD | 1.4 | No | Yes | Primary lung tumor (surgical resection) | Before T-DXd |
| 25 | Male | 61 | A775_G776insYVMA | PR | 4.4 | No | Yes | Primary lung tumor (biopsy) | Before T-DXd |

**Supplemental Figure S4**
Clinical characteristics, treatment outcomes, and tumor specimen information of patients with HER2-mutant NSCLC treated with T-DXd. Clinical characteristics, treatment history, best overall response (BOR), progression-free survival (PFS), and tumor specimen information of patients with HER2-mutant non-small cell lung cancer (NSCLC) who received trastuzumab deruxtecan (T-DXd). PFS was calculated from the initiation of T-DXd treatment to disease progression or death, whichever occurred first, or censored at the last disease assessment. Patients without disease progression or death at the data cutoff were censored at the date of their last disease assessment. Tumor specimen types and biopsy timing relative to systemic treatment are indicated. For patients with multiple tumor specimens, the corresponding specimen types and collection times are listed separately.

BOR, best overall response; Chemo, chemotherapy; ICI, immune checkpoint inhibitor; PD, progressive disease; PFS, progression-free survival; PR, partial response; SD, stable disease; T-DXd, trastuzumab deruxtecan.

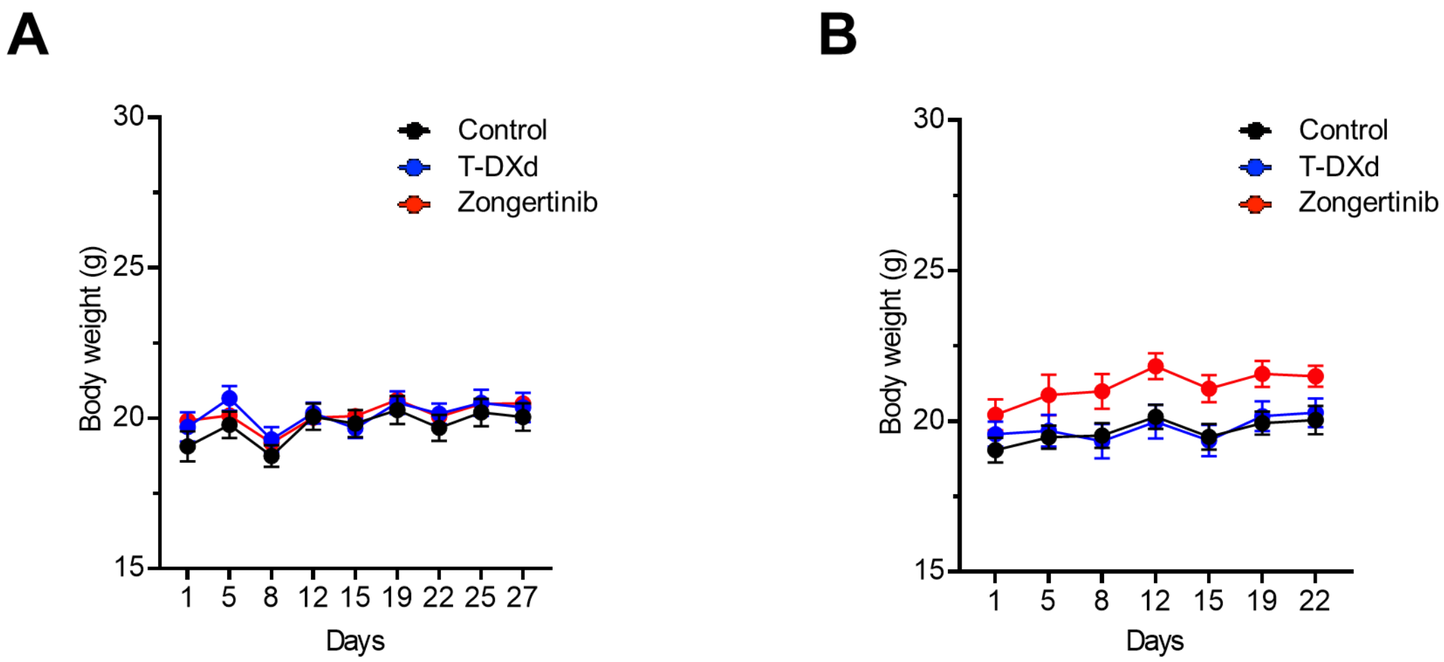
# Supplementary Fig. S5




**Supplemental Figure S5**
Clinical treatment timelines and tumor specimen collection in patients 3 and 5 with HER2-mutant NSCLC. Schematic timelines showing the clinical treatment courses and timing of tumor specimen collection in patients 3 (upper panel) and 5 (lower panel). Both patients received trastuzumab deruxtecan (T-DXd) followed by zongertinib after developing resistance to T-DXd. BCRP expression was assessed by immunohistochemistry in tumor specimens collected before and after T-DXd treatment. BCRP expression increased from 1+ to 3+ in both patients. Patient-derived organoids were established from specimens collected after T-DXd resistance, as indicated by blue arrows. The treatment-line numbers for T-DXd and zongertinib are indicated.

LUAD, lung adenocarcinoma; BCRR, breast cancer resistance protein; CBDCA, carboplatin; PEM, pemetrexed; IPI, ipilimumab; DOC, docetaxel; RAM, ramucirumab; T-DXd, trastuzumab deruxtecan; BOR, best overall response; PR, partial response; SD, stable disease; PFS, progression-free survival;

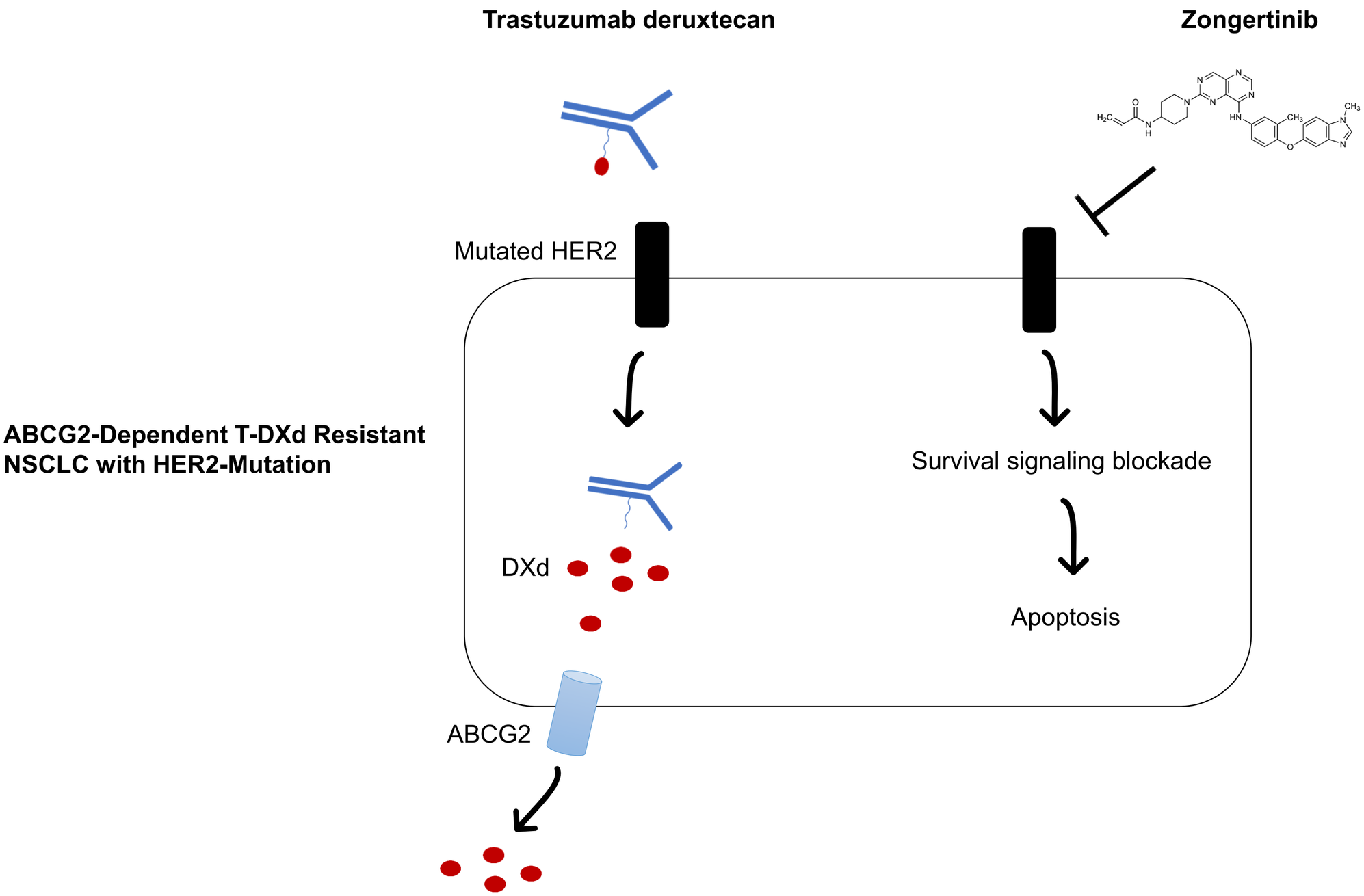
# Supplementary Fig. S6




**Supplemental Figure S6**
Body weights changes in xenograft mouse models of H1781 (A) and H1781DSR3 (B). Mice received T-DXd (3 mg/kg, single intraperitoneal injection on day 1), zongertinib (10 mg/kg, orally once daily on weekdays from day 1 until the final tumor measurement), or vehicle control (n = 10 mice per group). Data represent the mean ± SEM.

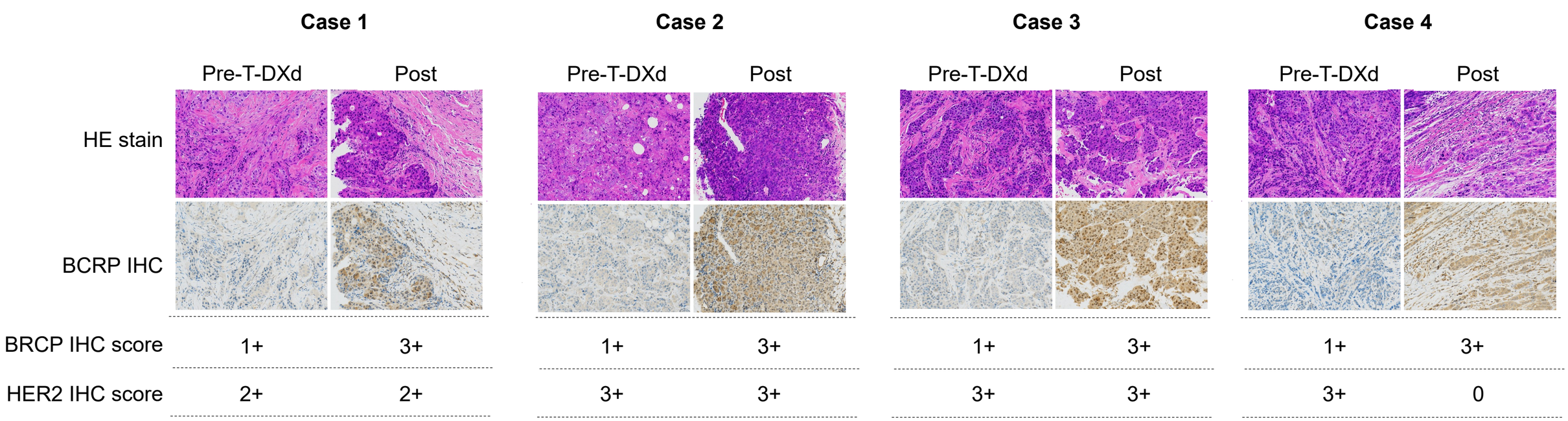
T-DXd, trastuzumab deruxtecan; SEM, standard error of the mean.

# Supplementary Fig. S7




**Supplemental Figure S7**
Schematic diagram illustrating the mechanism of action of trastuzumab deruxtecan (T-DXd) and zongertinib in ABCG2-dependent, T-DXd-resistant HER2-mutant non-small cell lung cancer (NSCLC)

# Supplementary Fig. S8




**Supplemental Figure S8**
ABCG2 immunohistochemistry according to HER2-positive breast cancer tumors obtained from patients prior to or after the development of resistance to T-DXd. IHC of ABCG2, HE staining, and HER2 IHC score was shown in pre- and post-T-DXd treatment samples.

# Supplementary Fig. S9

(A) Antibodies

| Target | Clone | Host | Supplier | Catalog number | Working dilution or antibody amount | RRID | Purpose |
|---|---|---|---|---|---|---|---|
| Cleaved PARP (Asp 214) | Monoclonal, D64E10 | Rabbit | Cell Signaling Technology | 5625 | 1:1000 | AB_10699459 | WB |
| Cleaved Caspase-3 (Asp 175) | Polyclonal | Rabbit | Cell Signaling Technology | 9661 | 1:1000 | AB_2341188 | WB |
| Actin | Polyclonal | Rabbit | Sigma-Aldrich | A2066 | 1:100 | AB_476693 | WB |
| Phospho-HER2/ErbB2 (Tyr1221/1222) | Monoclonal, 6B12 | Rabbit | Cell Signaling Technology | 2243 | 1:1000 | AB_490899 | WB |
| HER2/ErbB2 (29D8) Rabbit mAb | Monoclonal, 29D8 | Rabbit | Cell Signaling Technology | 2165 | 1:1000 | AB10692490 | WB |
| Phospho-p44/42 MAPK (Erk1/2) (Thr 202/Tyr 204) | Monoclonal, 20G11 | Rabbit | Cell Signaling Technology | 4376 | 1:1000 | AB-331772 | WB |
| p44/42 MAPK (Erk1/2) | Polyclonal | Rabbit | Cell Signaling Technology | 9102 | 1:1000 | AB_330744 | WB |
| Histone H2AX | Polyclonal | Rabbit | Abcam | ab11175 | 1:10000 | AB_297814 | WB |
| Phosho-Histone H2AX (Ser139) | Monoclonal, JBW301 | Mouse | Millipore | 05-636-I | 1:1000 | AB_2755003 | WB |
| ABCG2 | Monoclonal, D5V2K | Rabbit | Cell Signaling Technology | 42078 | 1:1000 | AB_2799211 | WB |
| AKR1C1/2/3 | Monoclonal, EPR16725 | Rabbit | Abcam | ab203834 | 1:5000 | AB_2927892 | WB |
| Phospho Akt (Ser473) | Recombinant monoclonal, D9E | Rabbit | Cell Signaling Technology | 4060 | 1:1000 | AB_23150149 | WB |
| Akt (pan) (C67E7) Rabbit mAb | Monoclonal, C67E7 | Rabbit | Cell Signaling Technology | 4691 | 1:1000 | AB_915783 | WB |
| CD340 | Monoclonal, 24D2 | Mouse | BioLegend | 324401 | 0.125µg/per million cells | AB_756117 | FCM |
| Purified Mouse IgG1, κ Isotype Control | Monoclonal, MG1-45 | Mouse | BioLegend | 401401 | 0.125µg/per million cells | AB_2801452 | FCM |
| BCRP/ABCG2 antibody [BXP-21] | Monoclonal, BXP-21 | Mouse | Abcam | ab3380 | 1:50 | AB_303758 | IHC |
| HER2/ErbB2 (29D8) Rabbit mAb | Monoclonal, 4B5 | Rabbit | Roche Diagnostics USA | 790-4493 | Ready-to-use (RTU) | AB_3101913 | IHC |

(B) Chemicals

| Chemicals | Supplier | Catalog number |
|---|---|---|
| Trastuzumab deruxtecan (T-DXd) | Daiichi Sankyo | Not applicable |
| DXd | Med ChemExpress | HY-13631D |
| Zongertinib | Boehringer Ingelheim | Not applicable |
| Febuxostat | Selleck Chemicals | S1547 |
| Ko143 | Selleck Chemicals | S7043 |

(C) Cell lines

| Cell line | Source | Identifier | RRID |
|---|---|---|---|
| NCI-H1781 | ATCC | CRL-5894 | CVCL_1494 |
| NCI-H2170 | ATCC | CRL-5928 | CVCL_1535 |

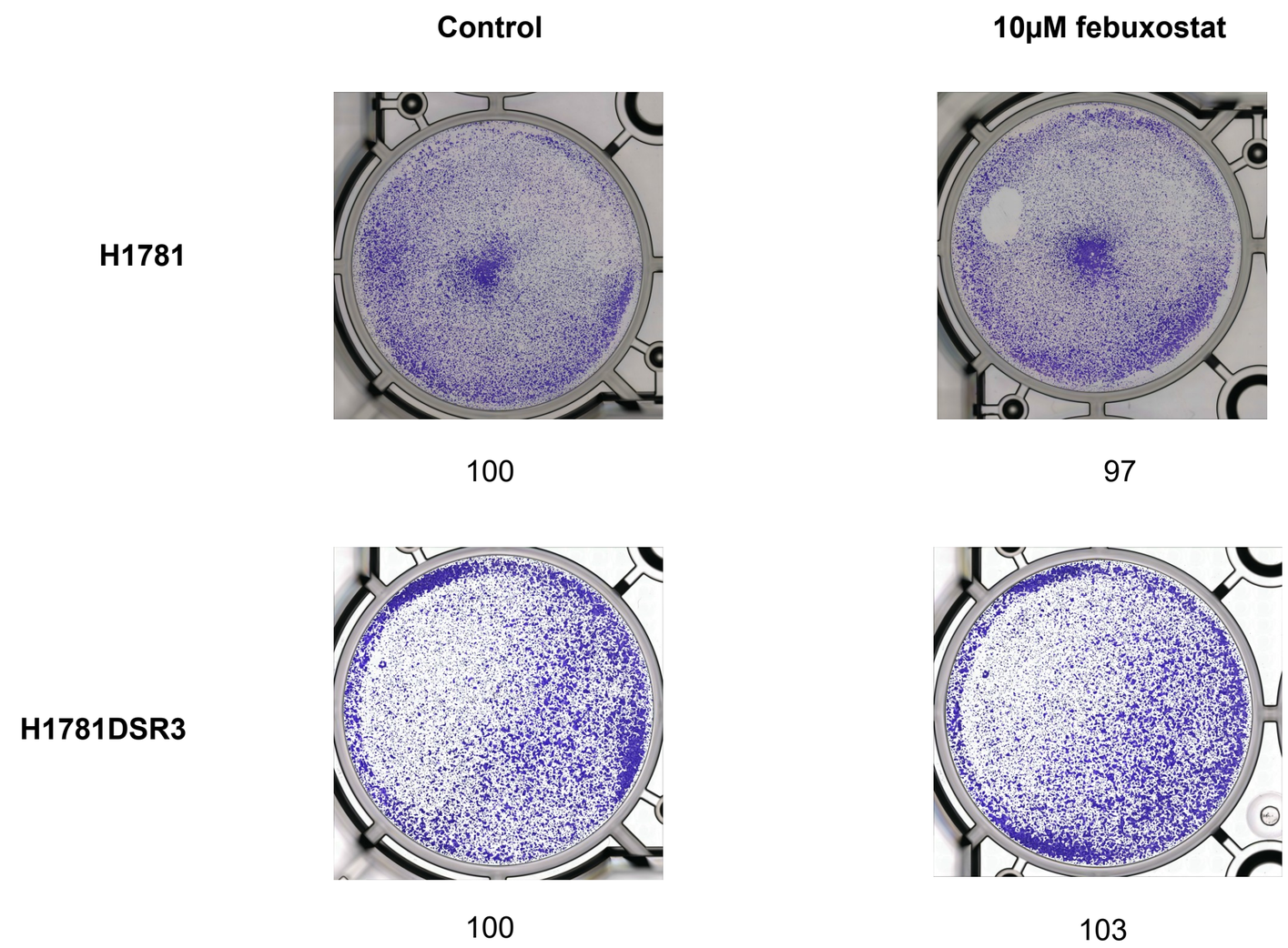
(D) Organoid culture reagents

| Reagemts | Source | Final concentration | Catalog number |
|---|---|---|---|
| Advanced DMEM/F12 | Thermo Fisher Scientific | - | 12634028 |
| Penicillin/Streptomycin | FUJIFILM Wako Pure Chemical Corporation | 1% | 161-20181 |
| Glutamax | Thermo Fisher Scientific | 2mM | 35050-061 |
| HEPES | Gibco, ThermoFisher Scientific | 10mM | 15630080 |
| B-27 | Thermo Fisher Scientific | 1× | 17504044 |
| Primocin | InvivoGen | 50 mg/ml | ant-pm-05 |
| N-Acetyl-L-cysteine | FUJIFILM Wako Pure Chemical Corporation | 1.25mM | A9165 |
| Human Recombinant EGF | PeproTech | 50ng/mL | AF-100-15 |
| FGF7 | PeproTech | 25ng/mL | 100-19 |
| FGF-10 | PeproTech | 100ng/mL | 100-26 |
| Y-27632 (ROCK inhibitor) | FUJIFILM Wako Pure Chemical Corporation | 5µM | 036-24023 |
| A-83-01 (TGF-β/Smad inhibitor) | Sigma-Aldrich | 500nM | SML0788 |
| SB202190 (p38 MAPK inhibitor) | Sigma-Aldrich | 500nM | S7067 |
| Nicotinamide | Sigma-Aldrich | 5mM | N0636 |
| Noggin | PeproTech | 100ng/mL | 120-10C |
| R-Spondin-1 | PeproTech | 500ng/mL | 120-38 |

**Supplemental Figure S9**
Antibodies, chemicals, cell lines, and organoid culture reagents used in this study. Details of the (A) antibodies, (B) chemicals, (C) cell lines, and (D) reagents used for patient-derived organoid culture are provided. For antibodies, the target, clone, host species, supplier, catalog number, working dilution or antibody amount, Research Resource Identifier (RRID), and experimental application are indicated. For chemicals, the supplier and catalog number are listed. Cell lines are identified by their source, catalog identifier, and RRID. The composition of the organoid culture medium is presented with the supplier, catalog number, and final concentration of each reagent.

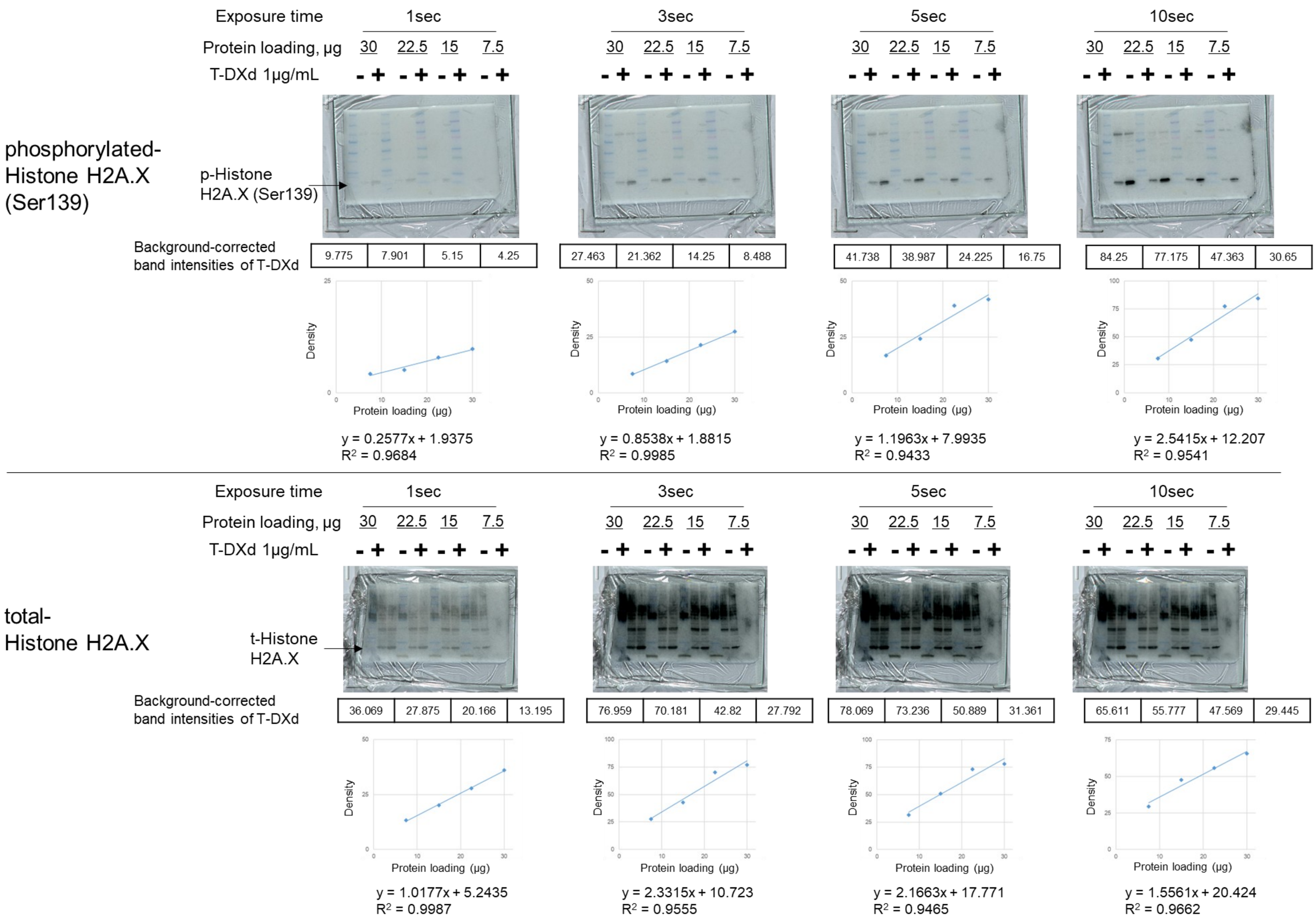
FCM, flow cytometry; IHC, immunohistochemistry; RRID, Research Resource Identifier; RTU, ready-to-use; WB, western blotting.

# Supplementary Fig. S10




**Supplementary Fig. S10**
Effects of febuxostat alone on the growth of H1781 and H1781DSR3 cells. Representative images from two independent high-density growth assays showing H1781 and H1781DSR3 cells treated with or without 10 μM febuxostat for 14 days. Cells were seeded in 6-well plates at a density of $3.0 \times 10^5$ cells per well and treated with febuxostat after 24 h. After 14 days, cells were fixed and stained with 0.5% crystal violet. Crystal violet-stained areas were quantified using ImageJ software, as described in Materials and Methods. The numbers below the images indicate the crystal violet-stained area relative to that of the corresponding untreated control (% of control).

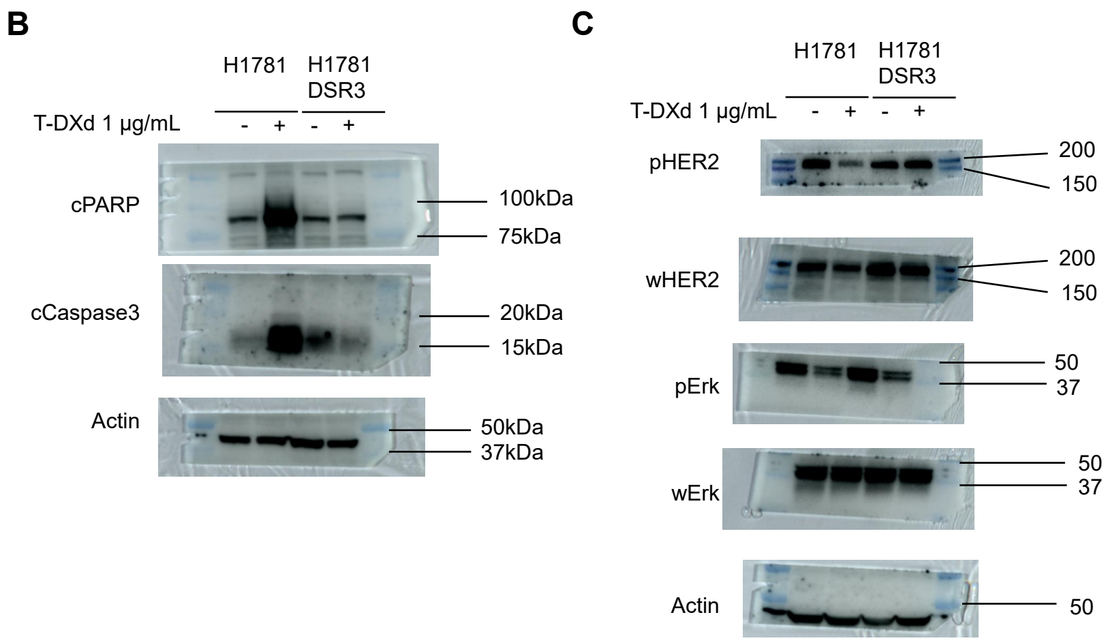
# Supplementary Fig. S11



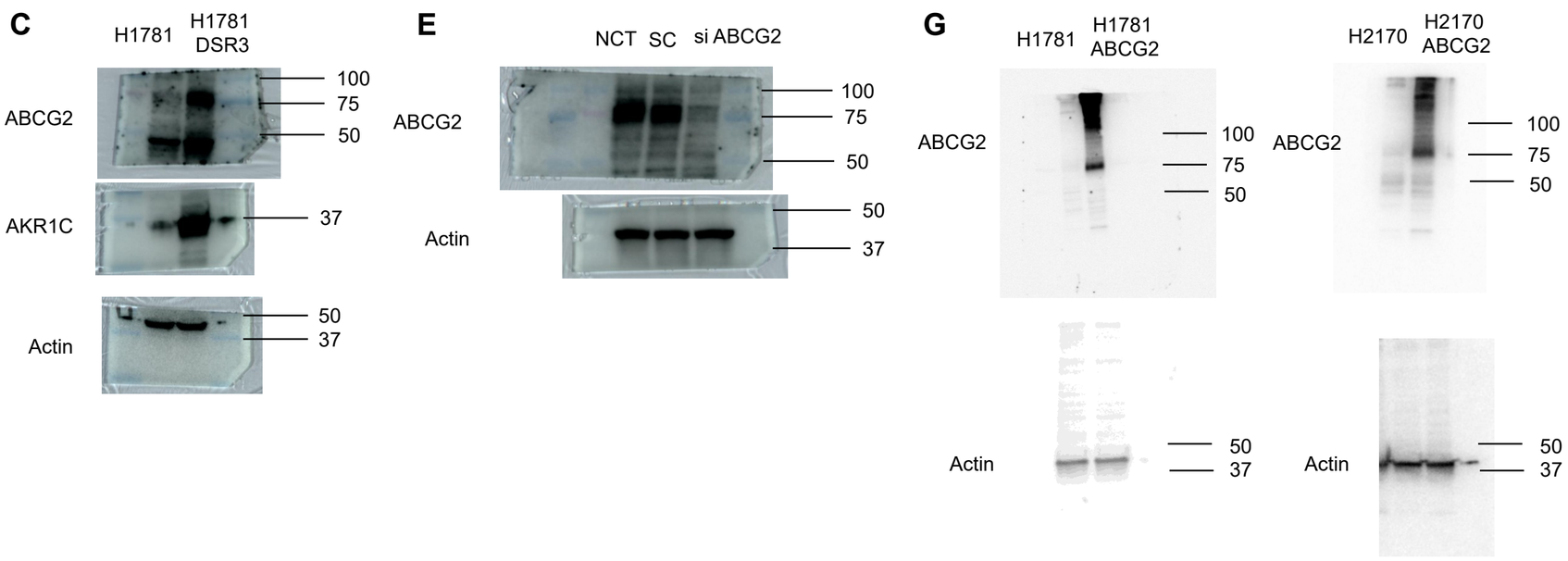

**Supplementary Figure S11**
Validation of the quantitative detection range for Histone H2A.X immunoblotting. Representative immunoblot images of phosphorylated Histone H2A.X (Ser139; upper panels) and total Histone H2A.X (lower panels) obtained using serial dilutions of protein lysates (7.5, 15, 22.5, and 30 µg) at the indicated exposure times. Background-corrected band intensities were plotted against protein loading. Linear regression analysis was performed, and the coefficient of determination ($R^2$) was calculated for each exposure condition to assess the linearity of signal detection.

# Supplementary Fig. S12

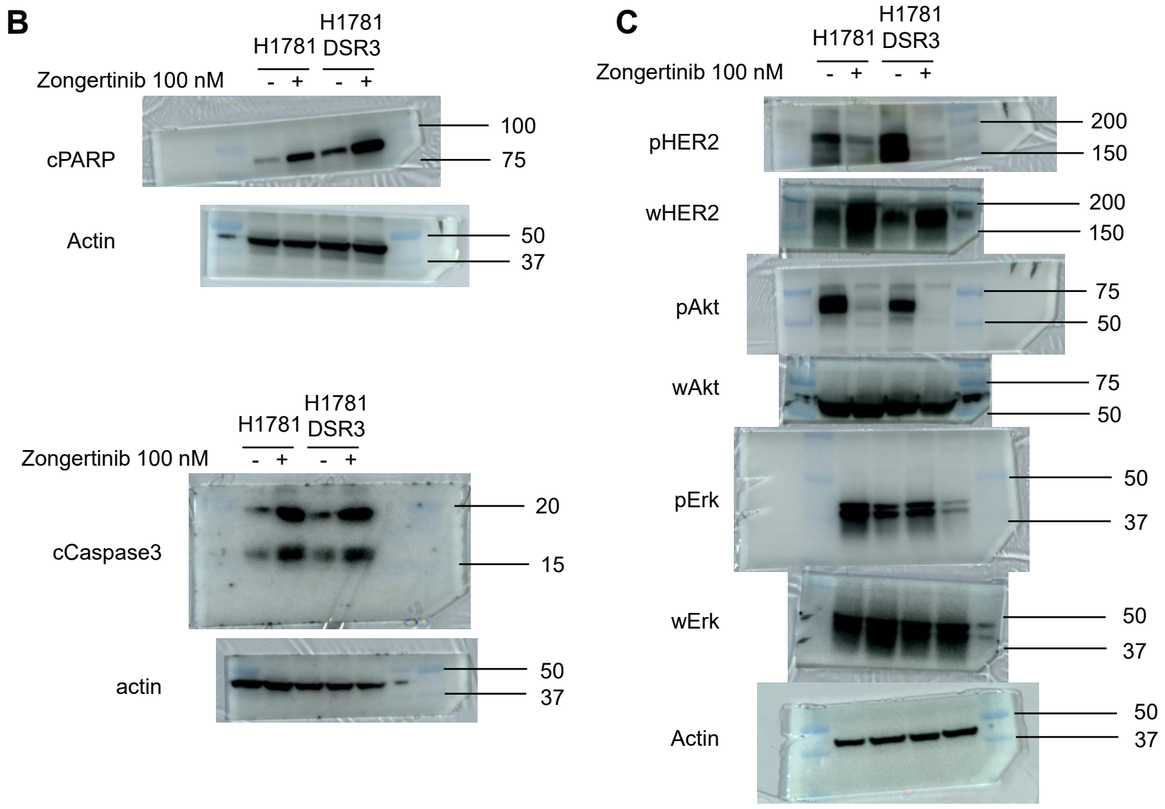
## Fig. 1



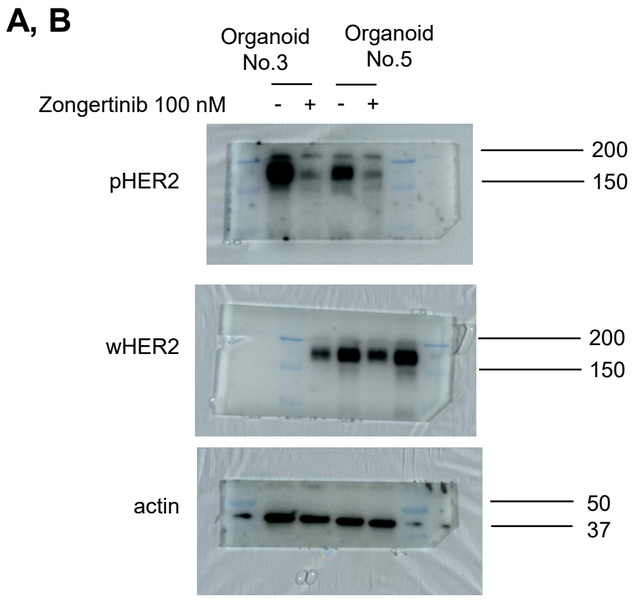

## Fig. 2




## Fig. 5




## Fig. 6




**Supplementary Figure S12**

Original uncropped western blot images used in this study.

Original uncropped western blot images corresponding to the immunoblot analyses presented in the main figures. The images show the original membranes used to detect the indicated proteins, including phosphorylated and total proteins and loading controls. Molecular weight markers are indicated where available. The corresponding protein targets and experimental conditions are identified for each blot.